http://dx.doi.org/10.21577/0103-5053.20190177

J. Braz. Chem. Soc., Vol. 31, No. 2, 305-312, 2020
Printed in Brazil - ©2020 Sociedade Brasileira de Química

Article

A Highly Selective Colorimetric Sensor for Cysteine Detection

Mengjiao Peng, *[a] *Hui Wang,*[b] *Gregory L. Gibson,*[c] *Hua Shang,*[a] *Jianmin Yang,*[a] *Yan Chen*[a] *and Yin Lu*[a]

[a]*Department of Chemical Engineering and Textile, Shaanxi Polytechnic Institute, 712000 Xianyang, Shaanxi, P. R. China*

[b]*Key Laboratory of Synthetic and Natural Functional Molecule Chemistry of Ministry of Education, College of Chemistry and Materials Science, Northwest University, 710069 Xi'an, Shaanxi, P. R. China*

[c]*Faculty of Science and Technology, Douglas College, V3M 5Z5 New Westminster, British Columbia, Canada*

Introducing a hybrid xanthene as a fluorophore, an 'ensemble'-based fluorescent sensor (*E*)-2-(6-(diethylamino)-2-((2-hydroxyphenylimino)methyl)-3-oxo-3*H*-xanthen-9-yl)benzoic acid (**a**) was designed and synthesised for detection of cysteine. Cysteine can release Cu^{II} ion from the non-fluorescent **a**-Cu^{II} complex. Then hydrolytic cleavage of Schiff base **a** produces a pink fluorescent compound 2-(6-(diethylamino)-2-formyl-3-oxo-3*H*-xanthen-9-yl)benzoic acid (**2**). We call this process a fluorescence off-on change. An obvious color change from purple **a** to pink **2** can be easily observed by the naked-eye. The calibration curve showed that the fluorescence intensity at 560 nm linearly increased over the cysteine concentration range of 0.379-100 μmol L^{-1} with a limit of detection of 0.379 μmol L^{-1}. Sensor **a**-Cu^{II} displayed excellent selectivity for cysteine, even homocysteine and glutathione did not show influence. The sensor was also used for detecting cysteine in human breast adenocarcinoma cells, which illustrates the practical value. Overall, the sensor appears to be useful for rapid, convenient and selective cysteine detection in living tissues.

Keywords: fluorescent sensor, cysteine detection, colorimetric, high selectivity

Introduction

Biological thiols including cysteine (Cys), glutathione (GSH), and homocysteine (Hcy) are vital to the cellular antioxidant defense system.[1,2] Cys plays an important role in protein synthesis, metabolism, and detoxification. High Cys content is related to neurotoxicity,[3] while low Cys content is involved in growth retardation, edema, hair depigmentation, pigmentation, liver injury, muscle and fat loss, skin damage, and weakness.[4] What's more, reduced Cys content is observed in patients infected with human immunodeficiency virus (HIV).[5,6] Because Cys level specifically is associated with different diseases, its discrimination from Hcy and GSH is necessary.

As fluorescent sensors possess advantages of simplicity, highly selectivity, and suitability for sensing in biological samples, they have become powerful tools to detect biological thiols. Thus, chemists have made considerable efforts to develop them for many applications including detect thiol species in living tissues.[7-17] The detection mechanism of reported fluorescent sensors include de-metalization from Cu^{II}-complex,[12-15] Michael addition,[18-28] cleavages of disulfide,[29-42] and excited-stated intramolecular proton transfer (ESIPT) mechanism.[43] De-metalization from Cu^{II}-complex attractted attention of chemists for its fast response time and obvious fluorescence change. But, it still exists as a challenge to distinguish Cys among biothiols as they share similar structures and reactivities. To solve this problem, considerable efforts have been made to the improve fluorescent sensors that respond selectively to Cys. A poly(methacrylic acid) (PMAA)-stabilized Ag clusters "on-off" sensor was established as Cys reacted directly with Ag clusters via the strong Ag–S interaction.[44] Fluorescent polymer sensor with silica particles as recognitition group can also achieve fluorescence quenching recognition in alcoholic media.[45] Graphene derivatives[46-48] with metallized

*e-mail: dream_vivi@163.com

deoxyribonucleic acid (DNA) can be used as an assembled sensor which makes "off-on" signal change possible for Cys detection. Ag-Pd bimetallic nanoparticles can detect Cys selectively due to the intrinsic effects of the nanocomposite.[49] Thermotropic liquid crystals in the gold grid can detect Cys based on the enzymatic reaction.[50] Tian *et al.*[51] reported a photo-induced electron transfer (PET)-based sensor HOTA. It can react with Cys by forming a 7-membered ring, which is impossible for GSH, thus high selectivity can be achieved. These methods supply direct and selective ways to detect Cys. Unfortunately, some inherent drawbacks such as water insoluble detection media, relatively long reaction times and single signal change limit their application in living tissues.

In the present work, we designed and synthesized (*E*)-2-(6-(diethylamino)-2-((2-hydroxyphenylimino) methyl)-3-oxo-3*H*-xanthen-9-yl)benzoic acid (**a**) as a fluorescence sensor for Cys detection. De-metalization from Cu^{II}-complex was used as detection mechanism for its fast response time and obvious fluorescence change. To avoid interference from other thiol species, hybrid xanthene was used as fluorophore to supply recognition site just for Cys. Obvious color change which can be easily observed by naked eye is also achieved as this fluorophore possesses a long emission wavelength. Water solubility of the sensor can be improved by metal ionic pairs. The key features of the novel colorimetric sensor include high selectivity, rapid detection and water soluble detection media suitable for live imaging, which can avoid the reported limitations.

Experimental

Materials and methods

All solvents and reagents were purchased from a commercial source (Xi'an, China) and used untreated. Absorption spectra were recorded on a Shimadzu UV-1700 spectrophotometer. Fluorescent spectra were taken on a Hitachi F-4500 fluorescence spectrophotometer. Mass spectra were collected on UltiMate3000 mass spectrometer. Nuclear magnetic resonance (NMR) spectra were obtained on a Varian Inova 400 spectrometer at 400 MHz for ^{1}H NMR and 100 MHz for ^{13}C NMR. Fourier tranform infrared (FTIR) spectra were tested in KBr pellets on a Bruker Equinox 55 FTIR spectrometer. Fluorescence images were taken on Olympus FV1000 confocal microscope.

Synthesis

The synthetic procedure of sensor **a** and (*E*)-2-(6-(diethylamino)-3-oxo-2-((phenylimino)methyl)-3*H*-xanthen-9-yl)benzoic acid (compound **b**) is shown in Scheme 1. The details can be found in the Supplementary Information (SI) section.

Preparation of MCF-7 breast carcinoma cells

The cell viability data were collected by performing

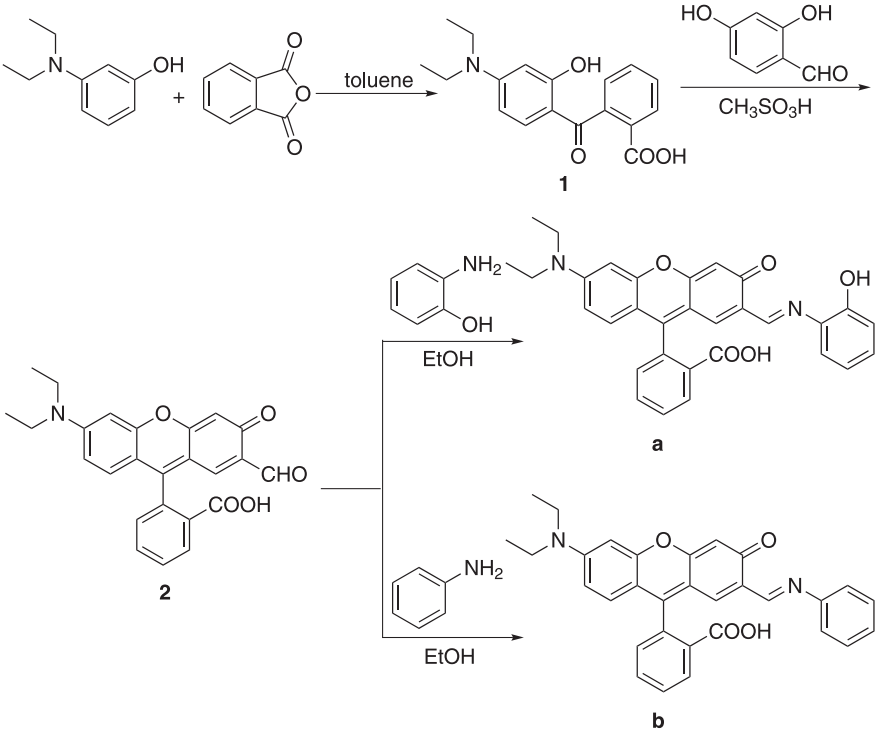

Scheme 1. Synthetic procedure of sensor **a** and compound **b**.

3-(4,5-dimethylthiazol-2-yl)-2,5 diphenyltetrazolium bromide (MTT) assays as shown in Figure S6 (SI section). The cells were incubated in Roswell Park Memorial Institute (RPMI) 1640 medium (Gibco) then supplemented with 10% fetal bovine serum (FBS; Gibco) at 37 °C in a damped atmosphere of 5% CO_2. For entire experiments, cells were obtained from subconfluent cultures by using trypsin 50 and were re-suspended in fresh complete medium before plating. *In vitro* cytotoxicity experiment was evaluated by using MTT reduction assays. In a typical operation, about 2000 cells were plated in 96-well plates for 24 h to permit the cells to adhere, and then incubated with **a**-Cu^{II} (20 μmol L^{-1}) in 5% CO_2 at 37 °C. At the termination of the cultured time, MTT solution (10 μL, 1 mg mL^{-1}) was added, and then the cells were cultured for another 4 h. Ultimately, the incubation solution was removed and dimethyl sulfoxide (DMSO, 150 μL) was added to each well. The absorbance of MTT was determined (λ = 488 nm) by using a microplate reader (BioTek, ELX808).

Spectral analyses

Deionized water was used throughout all experiments. Stock solutions (100.0 mmol L^{-1}) of the biological relevant analytes [amino acids: Cys, Hcy, GSH, glycine (Gly), glutamic acid (Glu), aspartic acid (Asp), methionine (Met), tyrosine (Tyr), alanine (Ala), leucine (Leu), isoleucine (Ile), threonine (Thr), serine (Ser), proline (Pro), arginine (Arg), histidine (His), tryptophan (Trp), lysine (Lys), valine (Val), phenylalanine (Phe)] were prepared in deionized water. Stocks of the sensor **a** and compound **b** (1.0 mmol L^{-1}) were prepared in ethanol. Stock solutions of **a**-Cu^{II} (0.5 mmol L^{-1}) were prepared in DMSO by mixing **a** and $Cu(ClO_4)_2$ with the ratio of 1:1.2. The stock solution of sensors was then deliquated to different concentration with the solution of dimethylformamide (DMF)-buffer (tris(hydroxymethyl) aminomethane (tris)-HCl, 1.0 mmol L^{-1}, pH 7.4, 1:1, v/v). The amino acids stock solution of 100.0 mmol L^{-1} was diluted to the corresponding concentrations with deionized water for spectra titration investigations. Spectra data were obtained in 20 min after addition at room temperature.

Results and Discussion

Even though thiol-promoted fluorescence from a nonfluorescent Cu^{II} complex has been applied as a chemosensing combination system,[11-14] its chemodosimetric function has rarely been discussed yet for thiol detection. Thus a novel fluorescent sensor **a** was designed and synthesized. Cysteine can release Cu^{II} ion from the non-fluorescent **a**-Cu^{II} complex. Then hydrolytic cleavage of the resulting Schiff base **a** produces a pink fluorescent compound **2**. We call this process a fluorescence off-on change (Scheme 2). Thus high sensitivity can be achieved owing to the affinity of cysteine for Cu^{II} ions. With this result we expand the methodologies for designing various fluorescent chemodosimeters. Moreover, this ensemble system achieved high selectivity toward Cys and colorimetric sensing recognizable by the naked eye. Additionally, we expect the Cu^{II} complex-based detection method to increase sensor water solubility due to the metal ionic pairs. Thus, highly selective visual Cys detection in biological systems can be achieved.

The C=N bond in Schiff bases is well known to be unstable in aqueous solution and is easily hydrolysed.[52] The time-dependent fluorescence of sensor **a** and compound **b** with and without the Cu^{II} ion in aqueous solution were studied (Figure S1, SI section). Without Cu^{II} ion, sensor **a** and compound **b** both hydrolyzed in 4 min and produced pink fluorescent **2**. When Cu^{II} ions are added to the system, the fluorescence intensity of sensor **a** decreased and the fluorescence intensity of compound **b** increased. This indicates that compound **b** was hydrolyzed but **a** was not. It is likely, then, that the *o*-OH group of sensor **a** provides a complex site for Cu^{II} that prevents further hydrolysis (Scheme 2). The maximum fluorescence emission wavelength of sensor **a** was 570 nm, which is typical of hybrid xanthene (Figure S2a, SI section). Upon addition of Cu^{II}, this fluorescence intensity at 570 nm decreased. This decreased fluorescence is likely due to a metal-ligand charge transfer (MLCT)-based heavy metal ion effect.[53,54] This is typically observed when Cu^{II} ions co-ordinate to a fluorescent compound. The maximum absorption wavelength of sensor **a** is 560 nm. With addition of Cu^{II}, the maximum absorption wavelength showed a blue shift to 540 nm. An isosbestic point is clear, which indicates generation of the **a**-Cu^{II} complex (Figure S2b, SI section). Critically, these changes occur when adding only 1 equiv. of Cu^{II}. The fluorescence emission spectrum of **a**-Cu^{II}, **a**-Cu^{II} + Cys, and compound **2** were compared (Figure S3, SI section). The **a**-Cu^{II} + Cys complex and compound **2** share almost the same emission spectrum, which indicates that the generated hydrolysis product is compound **2**. The complexing process between sensor **a** and Cu^{II} was also confirmed with a ^1H NMR titration experiment (Figure 1). When adding Cu^{II} (1.0 equiv.) to a DMSO-d_6-D_2O (1:1, v/v) solution of sensor **a**, the H_a signal disappeared while a set of new signals appeared in that area attributable to the **a**-Cu^{II} complex. The NMR spectrum of the hydrolysis product **2** is different from that of **a**-Cu^{II} showing the signal of H_b. The electrospray ionization mass spectrum (ESI-MS) (Figure 2) of the **a**-Cu^{II} complex makes it clear that the 1:1

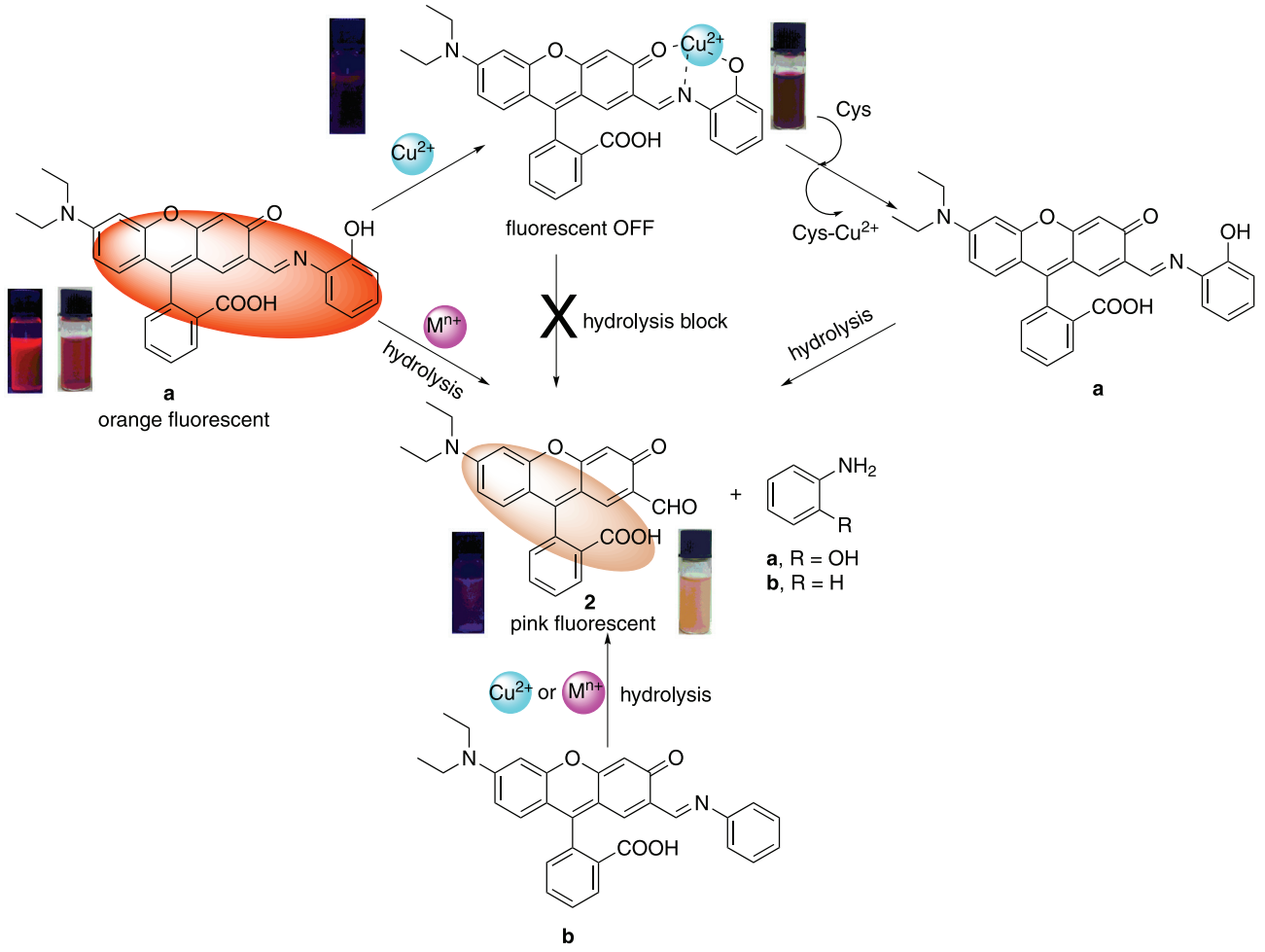

Scheme 2. The sensing mechanism of sensor **a** for Cys.

complex of **a** and Cu^{II} ion has been generated. Moreover, the generation of the hydrolyzate **2** was characterized by mass spectrometry, and the peak at *m/z* 416.1560 (calcd.: 416.1492) points out that hydrolyzate was produced.

In summary, the data indicate that Cys-induced decomplexation of Cu^{II} from the non-fluorescent **a**-Cu^{II} complex returns Schiff base **a**, and hydrolysis of **a** produces a fluorescent hybrid xanthene **2**. Fluorescence of **2** indicates the presence of Cys residues and the **a**-Cu^{II} complex functions as the sensor. Put in another way, Cys residues act as a "switch" in an off-on fluorescence system of **a**-Cu^{II} and **2**.

To demonstrate the selectivity of **a**-Cu^{II} for Cys in living media, fluorescence emission changes of **a**-Cu^{II} in aqueous solution were monitored upon addition of various amino acids, including Hcy and GSH (Figure 3a). Only **a**-Cu^{II} + Cys shows significant fluorescence, indicating selectivity of the **a**-Cu^{II} sensor for Cys specifically. This is remarkable because species reactive with Cys are also frequently reactive with Hcy and GSH. Given that both Hcy and GSH are larger than Cys, it is possible that only sterically small thiols such as Cys can remove Cu^{II} ions from the **a**-Cu^{II} complex. This method supplies a different way to distinguish Cys from Hcy and GSH which is not mentioned in the previous articles.[44-51] Competition experiments also demonstrate that **a**-Cu^{II} shows a highly selective response to Cys even in the presence of other amino acids (Figure 3b).

One attractive feature of this Cys sensor system is the clear visible emissions from both compounds **a** and **2** (Figure 4). The hybrid xanthene fluorophore was chosen specifically for its long emission wavelength that enables this colorimetric sensor system. Compound **a** has a markedly different red color from **2**, which is a distinct pink color. These distinct absorption and fluorescence changes make Cys detection possible with the naked eye. This is potentially more rapid and convenient than instrument-based detection methods[44-51] in some applications.

To gain insight into the detection of Cys with **a**-Cu^{II}, the fluorescence emission intensity was investigated (Figure 5). The free **a**-Cu^{II} exhibited a weak emission at 570 nm because of the MLCT-based heavy metal ion effect. By adding Cys, the emission shifted to a shorter

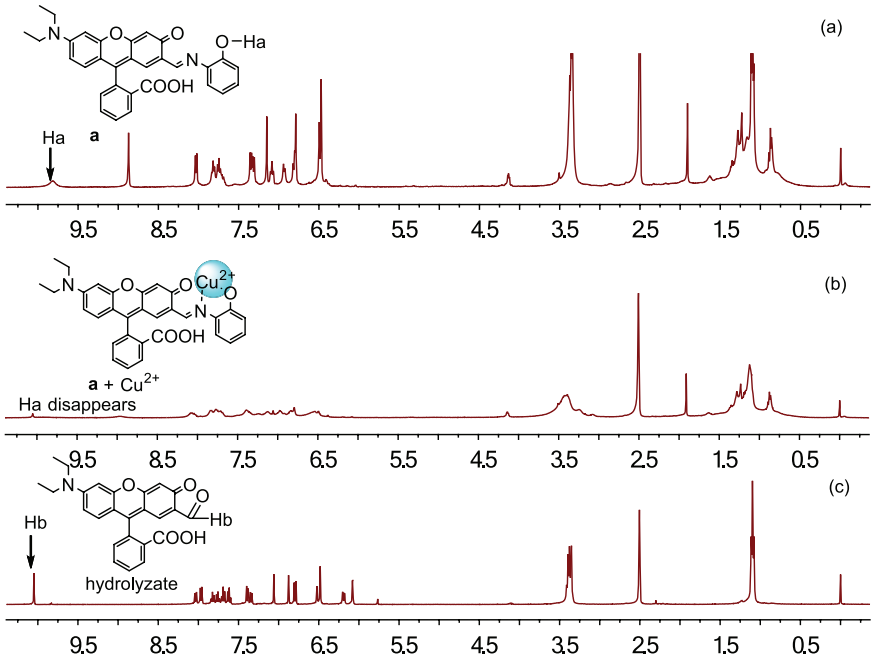

Figure 1. ^{1}H NMR spectra of **a** by adding Cu^{II} (1.0 equiv.) and Cys in DMSO-d_6-D_2O (1:1, v/v). (a) Synthesized **a**; (b) isolated **a**-Cu^{II}; and (c) the mixture of **a**-Cu^{II} in the presence of Cys.

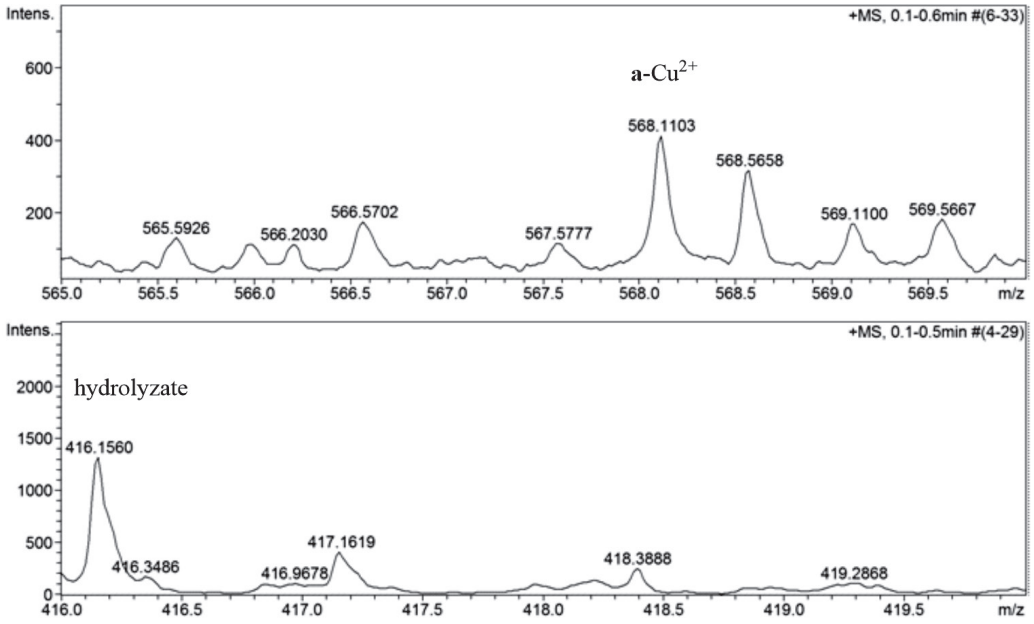

Figure 2. ESI-MS of **a**-Cu^{II} and hydrolyzate.

wavelength at 560 nm and the intensity increased gradually with increasing Cys concentration, indicating that Cu^{II} was removed from the **a**-Cu^{II}, after which the fluorescence of hybrid xathene **2** recovered. In fact, these changes in emission ceased and the fluorescence emission intensity at 560 nm became constant when the amount of Cys added reached 50 equiv. The stoichiometry of **a**-Cu^{II} and cysteine is 1:1, but **a**-Cu^{II} and cysteine cannot react completely when their ratio is 1:1, thus more cysteine is needed to move the reaction equilibrium toward the **a**-Cu^{II} complex dissociation direction. Under the same conditions, the fluorescence emission intensity changes made an excellent linear function with the concentration of Cys from 0 to 100.0 μmol L^{-1} (R^2 = 0.9986, Figure 6). This linear range can meet the requirement for cellular Cys detection which is similar to reported data.[42,49-51] The limit of detection (LOD) of **a**-Cu^{II} toward Cys is 3.79 × 10^{-7} mol L^{-1} in aqueous solutions according to 3σ / S (σ is the standard

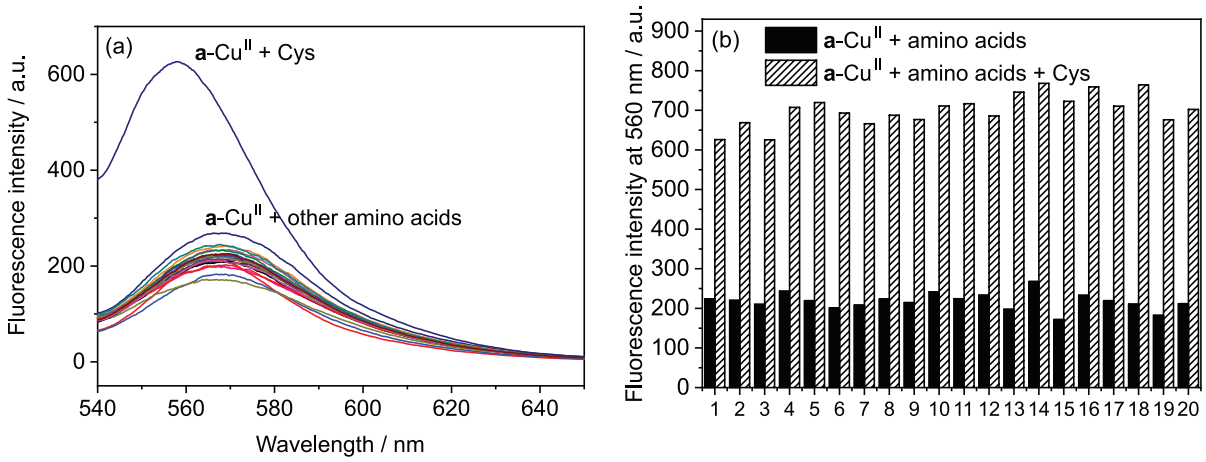

Figure 3. (a) Fluorescence intensity of **a**-Cu^{II} (2.0 μM) upon addition of 500 μM of multifarious species in DMF-buffer (tris-HCl, 1.0 mmol L^{-1}, pH 7.4, 1:1, v/v) (ex: 530 nm; em: 560 nm; slit = 2.5 / 5). (b) Competition graph; 1: blank / Cys, 2: Gly, 3: Glu, 4: Asp, 5: Met, 6: Tyr, 7: Ala, 8: Leu, 9: Ile, 10: Thr, 11: Ser, 12: Pro, 13: Arg, 14: His, 15: Trp, 16: Lys, 17: Val, 18: Phe, 19: Hcy, 20: GSH (reaction time: 20 min).

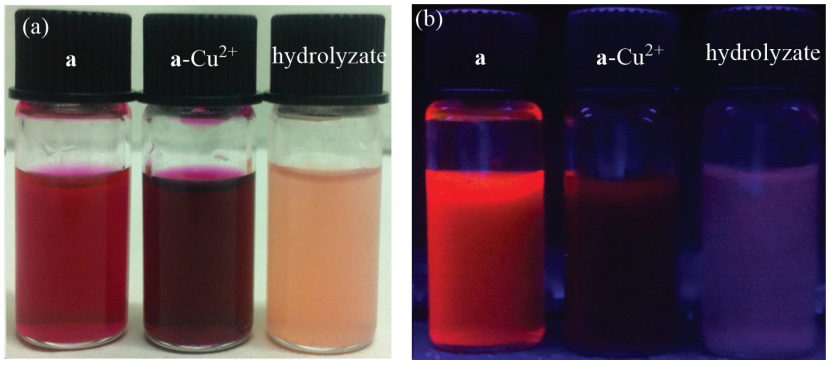

Figure 4. (a) Color and (b) fluorescence photoprints of **a**-Cu^{II} (0.5 mmol L^{-1}) in the absence (middle) and presence (right) of Cys (10 equiv.) in DMF-buffer (tris-HCl, 1.0 mmol L^{-1}, pH 7.4, 1:1, v/v). Excitation at 365 nm by an UV lamp after 20 min.

deviation and S is the slope). This phenomenon exhibits a relatively lower LOD comparing to literature LOD[42,49-51] (13.47-200 μmol L^{-1}). This indicated that **a**-Cu^{II} could be applied to quantitatively detect Cys concentration in a relatively wide range.

Then, the absorption spectrum changes of **a**-Cu^{II} (2.0 μmol L^{-1}) upon addition of different concentrations of Cys were investigated (Figure 7). Complex **a**-Cu^{II} exhibited an absorption peak at 550 nm. Upon addition of Cys to a solution of **a**-Cu^{II}, the absorption peak at 550 nm gradually increased and showed a blue shift to 530 nm, suggesting that Cu^{II} was removed from **a**-Cu^{II}. This is consistent with our hypothesized off-on fluorescence system.

To investigate the cell detecting ability of **a**-Cu^{II}, MCF-7 cells were developed with **a**-Cu^{II} (20 μmol L^{-1}) for 30 min at 37 °C, then washing by phosphate-buffered saline (PBS) solution to remove the residual compound **a**-Cu^{II} (Figure 8). Confocal imaging changes can be clearly observed. When a selective thiol modifying reagent *N*-ethylmaleimide (NEM) and **a**-Cu^{II} were raised with MCF-7 cells, the fluorescence image showed a dark fluorescence because Cys connected to

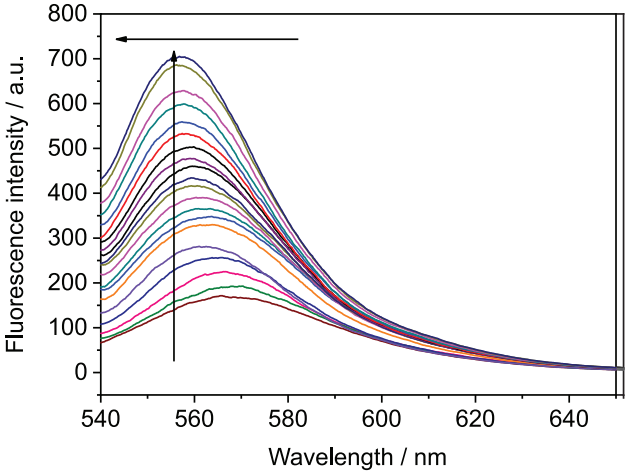

Figure 5. Changes in fluorescent intensity of **a**-Cu^{II} (2.0 μmol L^{-1}) measured in DMF-buffer (tris-HCl, 1.0 mmol L^{-1}, pH 7.4, 1:1, v/v) upon addition of Cys (ex: 530 nm; slit = 2.5 / 5). Cys concentration (from bottom to top): 0, 10, 20, 30, 40, 50, 60, 70, 80, 90, 100, 150, 180, 200, 250, 300, 350, 400, 450, 500 μmol L^{-1}.

NEM so that **a**-Cu^{II} kept resistance. When the concentration of NEM decreased, light pink fluorescence partly recovered

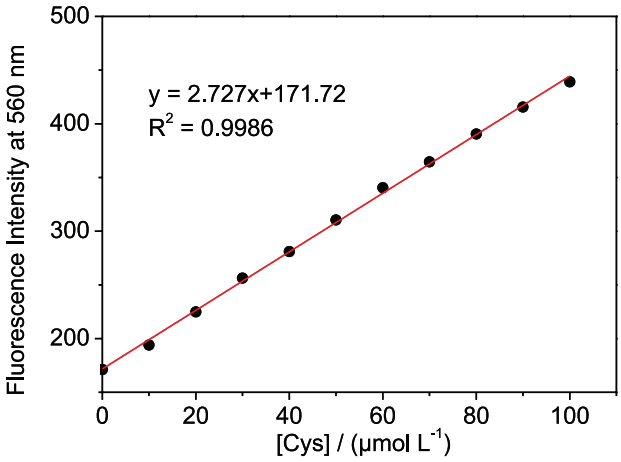

Figure 6. Fluorescent calibration curve of **a**-Cu^{II} (2.0 μmol L^{-1}) as a function of the concentration of Cys (all experiments were performed three times).

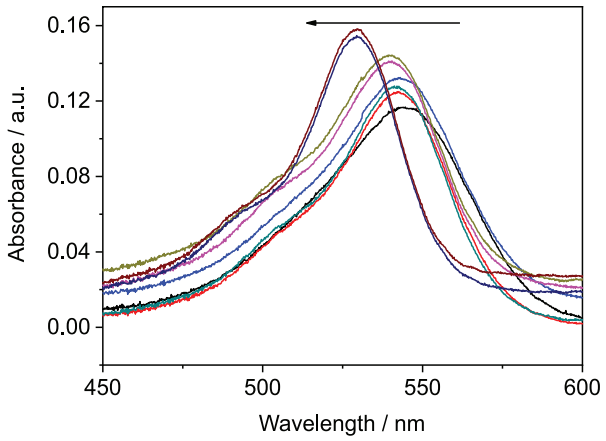

Figure 7. Changes in absorbance intensity of **a**-Cu^{II} (2.0 μmol L^{-1}) measured in DMF-buffer (tris-HCl, 1.0 mmol L^{-1}, pH 7.4, 1:1, v/v) upon addition of Cys. Cys concentration (from bottom to top): 0, 20, 40, 60, 80, 100, 250, 500 μmol L^{-1}.

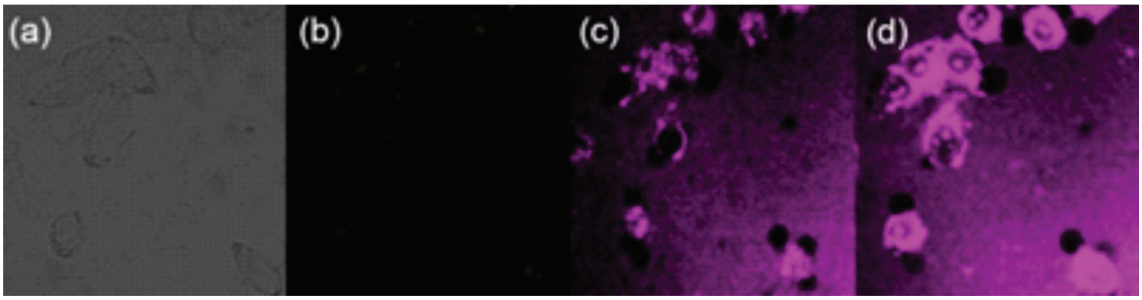

Figure 8. Confocal fluorescence images of sensor (Olympus FV1000). (a) Bright-field transmission image; (b) fluorescence image of cells incubated with 20 μmol L^{-1} of **a**-Cu^{II} and NEM (1000 μmol L^{-1}) (λex = 488 nm); (c) fluorescence image of cells incubated with 20 μmol L^{-1} of **a**-Cu^{II} and NEM (500 μmol L^{-1}) (λex = 488 nm); (d) fluorescence image of cells incubated with 20 μmol L^{-1} of **a**-Cu^{II} (λex = 488 nm).

because part of Cys in the cell released and reacted with **a**-Cu^{II}. Without NEM application, MCF-7 cells raised with **a**-Cu^{II} showed a light pink fluorescence image when excited at 488 nm. Thus, the sensor **a**-Cu^{II} can be used as a suitable fluorescence sensor for detecting Cys in live cells.

Conclusions

Generally speaking, the novel hybrid xanthene-Cu^{II} ensemble based sensor **a**-Cu^{II} shows high selectivity toward Cys at pH 7.4 under water-soluble environment. An 'off-on' fluorescence change of **a**-Cu^{II} was observed by addition of Cys. Cys addition leads to de-complexation of the Cu^{II} ion from fluorescent **a**, then hydrolytic cleavage of the produced Schiff base **a** produced a pink fluorescent hybrid xanthene **2**. Unlike reported de-metalization from Cu^{II}-complex mechanism, we use a hybrid xanthene as fluorophore to supply recognition site just for Cys and avoid interference from other thiol species. With the long emission wavelength of this fluorophore, this system achieves naked-eye and simple-to-use detection of Cys. Furthermore, this sensor system is highly biocompatible and is capable of emitting detectable fluorescence from within biological cells. Thus, the sensor seems to be a practical system for quickly, conveniently, and selectively detecting Cys in living tissues.

Supplementary Information

Supplementary information is available free of charge at http://jbcs.sbq.org.br as PDF file.

Acknowledgments

We are very grateful for the support of this work from the Special Foundation of the Education Committee of Shaanxi Province (No. 16JK1058).

References

1. Mascio, P. D.; Murphy, M. E.; Sies, H.; *Am. J. Clin. Nutr.* **1991**, *53*, 194S.
2. Zhang, S. Y.; Ong, C.-N.; Shen, H.-M.; *Cancer Lett.* **2004**, *208*, 143.
3. Wang, X. F.; Cynader, M. S.; *J. Neurosci.* **2001**, *21*, 3322.

4. Shahrokhian, S.; *Anal. Chem.* **2001**, *73*, 5972.
5. Zeng, Y. G.; Zhang, X. D.; Zhang, Q.; *Anal. Chim. Acta* **2008**, *627*, 254.
6. Huo, F.-J.; Sun, Y.-Q.; Su, J.; Chao, J.-B.; Zhi, H.-J.; Yin, C.-X.; *Org. Lett.* **2009**, *11*, 4918.
7. Sippel, T. O.; *J. Histochem. Cytochem.* **1981**, *29*, 314.
8. Rusin, O.; St. Luce, N. N.; Agbaria, R. A.; Escobedo, J. O.; Jiang, S.; Warner, I. M.; Dawan, F. B.; Lian, K.; Strongin, R. M.; *J. Am. Chem. Soc.* **2004**, *126*, 438.
9. Pires, M. M.; Chmielewski, J.; *Org. Lett.* **2008**, *10*, 837.
10. Wang, H.; Zhou, G.; Mao, C.; Chen, X.; *Dyes Pigm.* **2013**, *96*, 232.
11. Hudec, R.; Hamada, K.; Mikoshiba, K.; *Anal. Biochem.* **2013**, *433*, 95.
12. Yang, X.-F.; Liu, P.; Wang, L.; Zhao, M.; *J. Fluoresc.* **2008**, *18*, 453.
13. Hao, W.; McBride, A.; McBride, S.; Gao, J. P.; Wang, Z. Y.; *J. Mater. Chem.* **2011**, *21*, 1040.
14. Yang, Y.-K.; Shim, S.; Tae, J.; *Chem. Commun.* **2010**, *46*, 7766.
15. Jung, H. S.; Han, J. H.; Habata, Y.; Kang, C.; Kim, J. S.; *Chem. Commun.* **2011**, *47*, 5142.
16. Peng, M. J.; Yang, X. F.; Yin, B.; Guo, Y.; Suzenet, F.; En, D.; Li, J.; Li, C. W.; Duan, Y. W.; *Chem. - Asian J.* **2014**, *9*, 1817.
17. Da, E.; Guo, Y.; Chen, B. T.; Dong, B.; Peng, M. J.; *RSC Adv.* **2014**, *4*, 248.
18. Kwon, H.; Lee, K.; Kim, H. J.; *Chem. Commun.* **2011**, *47*, 1773.
19. Cho, A. Y.; Choi, K.; *Chem. Lett.* **2012**, *41*, 1611.
20. Liu, Y.; Yu, Y.; Lam, J. W. Y.; Hong, Y. N.; Faisal, M.; Yuan, W. Z.; Tang, B. Z.; *Chem. - Eur. J.* **2010**, *16*, 8433.
21. Jiang, W.; Fu, Q. Q.; Fan, H. Y.; Ho, J.; Wang, W.; *Angew. Chem.* **2007**, *119*, 8597.
22. Schyrr, B.; Pasche, S.; Voirin, G.; Weder, C.; Simon, Y. C.; Foster, E. J.; *ACS Appl. Mater. Interfaces* **2014**, *6*, 12674.
23. Lin, W. Y.; Yuan, L.; Cao, Z. M.; Feng, Y. M.; Long, L. L.; *Chem. - Eur. J.* **2009**, *15*, 5096.
24. Matsumoto, T.; Urano, Y.; Shoda, T.; Kojima, H.; Nagano, T.; *Org. Lett.* **2007**, *9*, 3375.
25. Li, X.; Huo, F.; Yue, Y.; *Sens. Actuators, B* **2017**, *253*, 42.
26. Chen, X. Q.; Ko, S.-K.; Kim, M. J.; Shin, I.; Yoon, J.; *Chem. Commun.* **2010**, *46*, 2751.
27. Qian, Y.; Karpus, J.; Kabil, O.; *Nat. Commun.* **2011**, *2*, 495.
28. Hong, V.; Kislukhin, A. A.; Finn, M. G.; *J. Am. Chem. Soc.* **2009**, *131*, 9986.
29. Hun, X.; Sun, W.; Zhu, H.; Du, F.; Liu, F.; Xu, Y.; *Chem. Commun.* **2013**, *49*, 9603.
30. Shiu, H. Y.; Chong, H. C. Y.; Leung, C.; Wong, M. K.; Che, C. M.; *Chem. - Eur. J.* **2010**, *16*, 3308.
31. Wang, F.; Zhou, L.; Zhao, C.; Wang, R.; Fei, Q.; Luo, F.; *Chem. Sci.* **2015**, *6*, 2584.
32. Shao, J. Y.; Guo, H. M.; Ji, S. M.; Zhao, J. Z.; *Biosens. Bioelectron.* **2011**, *26*, 3012.
33. Johnson, R. J.; Lin, S. R.; Raines, R. T.; *FEBS J.* **2010**, *273*, 5457.
34. Maeda, H.; Matsuno, H.; Ushida, M.; Katayama, K.; Saeki, K.; Itoh, N.; *Angew. Chem.* **2005**, *117*, 2982.
35. Wang, R.; Chen, L.; Liu, P.; Zhang, Q.; Wang, Y.; *Chem. - Eur. J.* **2012**, *18*, 11343.
36. Bouffard, J.; Kim, Y.; Swager, T. M.; Weissleder, R.; Hilderbrand, S. A.; *Org. Lett.* **2008**, *10*, 37.
37. Mertens, M. D.; Bierwisch, A.; Li, T.; Gütschow, M.; Thiermann, H.; Wille, T.; *Toxicol. Lett.* **2016**, *244*,161.
38. Lee, H.; Kim, H. J.; *Org. Biomol. Chem.* **2013**, *11*, 5012.
39. Zhang, J.; Yu, B.; Ning, L.; Zhu, X.; Wang, Z.; Chen, Z.; *Eur. J. Org. Chem.* **2015**, *2015*, 1711.
40. Tang, B.; Xing, Y. L.; Li, P.; Zhang, N.; Yu, F. B.; Yang, G. W.; *J. Am. Chem. Soc.* **2007**, *129*, 11666.
41. Alloza, I.; Martens, E.; Hawthorne, S.; *Anal. Biochem.* **2004**, *324*, 137.
42. Li, J.; Tian, C.; Yuan, Y.; Yang, Z.; Yin, C.; Jiang, R.; Song, W.; Li, X.; Lu, X.; Zhang, L.; Fan, Q.; Huang, W.; *Macromolecules* **2015**, *48*, 1017.
43. Wang, Y.; Zhu, M.; Jiang, E.; Hua, R.; Na, R.; Li, Q. X.; *Sci. Rep.* **2017**, *7*, 4377.
44. Shang, L.; Dong, S.; *Biosens. Bioelectron.* **2009**, *24*, 1569.
45. Jang, G.; Lee, T. S.; *Polym. Bull.* **2016**, *73*, 2447.
46. Xie, W. Y.; Huang, W. T.; Li, N. B.; Luo, H. Q.; *Chem. Commun.* **2012**, *48*, 82.
47. Lin, Y.; Yu, T.; Fang, P.; Ren, J.; Qu, X.; *Adv. Funct. Mater.* **2011**, *21*, 4565.
48. Li, Z.; Wang, Y.; Ni, Y.; Kokot, S.; *Sens. Actuators, B* **2015**, *207*, 490.
49. Murugavelu, M.; Karthikeyan, B.; *Superlattices Microstruct.* **2014**, *75*, 916.
50. Wang, Y.; Hu, Q.; Tian, T.; Gao, Y.; Yu, L.; *Colloids Surf., B* **2016**, *147*, 100.
51. Tian, M.; Guo, F.; Sun, Y.; Zhang, W.; Miao, F.; Liu, Y.; Song, G.; Ho, C.-L.; Yu, X.; Sun, J. Z.; Wong W.-Y.; *Org. Biomol. Chem.* **2014**, *12*, 6128.
52. Mandal, S.; Poria, D. K.; Seth, D. K.; Ray, P. S.; Gupta, P.; *Polyhedron* **2014**, *73*,12.
53. Kim, J. S.; Quang, D. T.; *Chem. Rev.* **2007**, *107*, 3780.
54. Jung, H. S.; Kwon, P. S.; Lee, J. W.; Kim, J. I.; Hong, C. S.; Kim, J. W.; Yan, S.; Lee, J. Y.; Lee, J. H.; Joo, T.; Kim, J. S.; *J. Am. Chem. Soc.* **2009**, *131*, 2008.

Submitted: March 20, 2019
Published online: July 30, 2019